6B.4 FIRST WIND MEASUREMENTS WITH THE METEOROLOGICAL UAV 'M^{2}AV CAROLO'

Aline van den Kroonenberg[1], Thomas Spieß and Jens Bange

Institute of Aerospace Systems at Technical University Braunschweig, Germany

1. INTRODUCTION

Aircraft measurements play an important role in boundary-layer research. The main advantage of airborne systems is their flexibility: capability of measuring on horizontal tracks or probing the boundary layer vertically by slant profiles. Due to the high operational speed an aircraft can obtain statistically significant measurements faster than ground-based measurement systems. Research aircraft are therefore involved in large field experiments as addition to ground stations and remote-sensing systems with area-representive measurements (e.g. Bange *et al.*, 2002; Beyrich and Mengelkamp, 2006). An important variable for boundary-layer research is the wind vector. The wind-vector calculation from airborne measurements is complex and described by many authors, mostly based on the studies of Axford (1968) and Lenschow (1986). The difference between the aircraft velocity relative to the earth (inertial velocity) and the velocity relative to the air (true airspeed) results in the wind vector. The wind vector is small compared to the true airspeed and the inertial velocity vectors, and is subject to the errors of the complex determination of these vectors (Grossman, 1977).

During the last ten years a new trend in the airborne meteorology evolves: the operation of mini unmanned aerial vehicles (UAV). The mini UAVs are inexpensive compared to a fully equipped research aircraft and highly flexible. The meteorological mini UAV 'M^{2}AV ' was developed at the Institute of Aerospace Systems (ILR = Institut für Luft- und Raumfahrtsysteme) at the Technical University of Braunschweig and build in cooperation with Mavionics GmbH, Braunschweig, Germany. The M^{2}AV is a twin engine (electric propulsion) aircraft with a wingspan of 2 m and a maximum take-off weight of 6 kg. The M^{2}AV is controlled by an on-board autopilot system. The M^{2}AV measures temperature, humidity and the wind vector and already successfully deployed in boundary-layer research campaigns (Fig. 1).

A long term co-operation between the ILR and the British Antarctic Survey (BAS) was established in 2005. A joint project was the deployment of one M^{2}AV to Halley station for the southern summer 2005/2006. Two additional systems and one researcher of ILR were sent in the southern summer 2006/2007 to Halley station. This paper will describe the method to determine the wind vector with the M^{2}AV and the measurement results from the Antarctica campaign 2007.

Fig. 1: *The measurement nose with the 5HP, Vaisala Intercap and Dantec foil temperature sensor mounted.*

2. M^{2}AV INSTRUMENTATION

The aircraft can be hand-launched or started with a bungee rope. After the take-off the way-point navigation is activated and the system flies autonomously. A laptop computer is used to follow the aircrafts mission and to check (meteorological) parameters which are send from the aircraft to the laptop using a radio link. Within the radio link, the mission can be changed by sending new way-points to the aircraft. Outside of the radio link range, the aircraft continues the commanded mission and can reach a flight distance of $60-70$ km (at an airspeed of 22 m s^{-1}). The landing procedure can be done automatically or manually. The detailed specifications were published by Buschmann *et al.* (2004) and Spieß *et al.* (2007), a summary is listed in Tab. 1.

The meteorological package consists of one fast temperature sensor (thin foil element) developed by Dantec and a Vaisala Intercap (HMP50) which measures the temperature and relative humidity with a response time (in flight) of 1 s. A five-hole probe (5HP) manufactured by the Institute

[1]Corresponding author: Aline van den Kroonenberg, e-mail: a.kroonenberg@tu-bs.de

Tab. 1: *Specification and performance of the M^2AV .*

Take off weight	6 kg
Wing span	2 m
Twin engine	electric propulsion
Navigation	GPS, IMU
Optimal speed	21-24 m s^{-1}
Max. climbing rate	5 m s^{-1}
Endurance	<60 min
Horizontal distance	60–70 km
Altitude range	10-800 m AGL

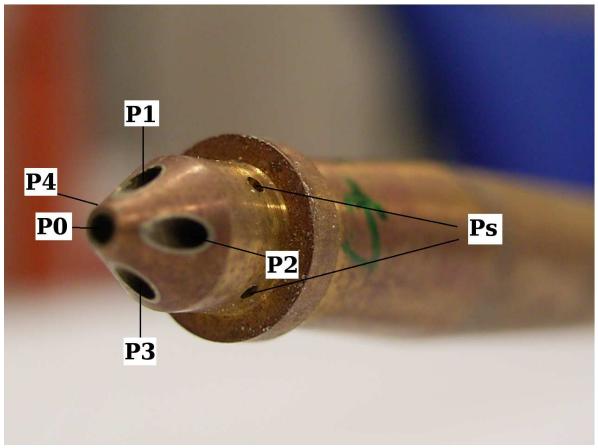

Fig. 2: *The 5HP with a diameter of 6 mm. The 4 smaller circumferential holes (only 2 visible) are the static pressure ports.*

of Fluid Dynamics (TU Braunschweig) measures five differential pressures at the tip of the probe (Fig. 2). The static pressure is measured by four holes at the side of the probe. The measurements are used to calculate the airflow angles and the dynamic pressure (see following paragraph). A micro-electromechanical sensor system (MEMS) gives time series of the angle accelerations and the accelerations in x, y and z direction and was developed at the ILR. The sensor block contains a 3-axis-IMU (inertial measurements unit), that consists of three angular-rate sensors with a range of $\pm 300^\circ$ s^{-1} and two accelerometers with two axes each, providing redundancy for the aircrafts longitudinal axis. The inertial velocity vector and the position are measured by a single-antenna single-frequency GPS receiver (μ-blox company, type SAM LS) with a measurement frequency of 1 Hz. Except for the GPS receiver, the IMU and the meteorological sensors are sampled with 100 Hz.

3. WIND VECTOR

The wind measurement by airborne systems is challenging. High resolution and thus fast and accurate sensors are needed to determine the attitude, position and the velocity of the aircraft relative to the earth, and the airflow at the nose of the fuselage with high accuracy.

The wind $\mathbf{W}_g$ defined in geodetic coordinate system is the vector difference between the inertial velocity $\mathbf{V}_g$ and the true airspeed $\mathbf{U}_a$ (neglecting the small lever-arm to the 5HP):

$$\mathbf{W}_g = \mathbf{V}_g + \mathbf{M}_{gb} \cdot \mathbf{M}_{ba} \cdot \mathbf{U}_a \quad , \tag{1}$$

with the matrix $\mathbf{M}_{ba}$ to transform the true airspeed from aerodynamic (index 'a') into body (index 'b') coordinates, and $\mathbf{M}_{gb}$ for the transformation into the geodetic coordinate system (index 'g'). Figure 3 shows all the needed aircraft coordinate system.

To obtain all components of (1) in the geodetic coordinate system, two coordinate transformation have to be applied. First, the true airspeed vector $\mathbf{U}_a$ as measured in the aerodynamic coordinate system has to be transformed into the body coordinate system of the aircraft using the transformation according to Boiffier (1998), Lenschow (1986) and Axford (1968)

$$\mathbf{U}_b = \mathbf{M}_{ba} \cdot \mathbf{U}_a = \frac{|\mathbf{U}_a|}{D} \cdot \begin{bmatrix} 1 \\ \tan\beta \\ \tan\alpha \end{bmatrix} \tag{2}$$

with a normalization factor

$$D = \sqrt{1 + \tan^2\alpha + \tan^2\beta} \tag{3}$$

and the angles α, β (measured by the 5HP in flight) between the airflow and the x-axis and z-axis in body coordinate system, respectively. The norm $|\mathbf{U}_a|$ has to be calculated using the measured total air temperature T_{tot}, the static pressure p and the dynamic pressure q

$$|\mathbf{U}_a|^2 = 2 \cdot c_p \cdot T_{\mathrm{tot}} \cdot \left[1 - \left(\frac{p}{p+q}\right)^{\kappa}\right] \quad , \tag{4}$$

with the poisson number $\kappa = R/c_p$ where $R = 287\ \mathrm{J \cdot K^{-1} \cdot kg^{-1}}$ is the gas constant for dry air and $c_p = 1005\ \mathrm{J \cdot kg^{-1} \cdot K^{-1}}$ the specific heat for dry air.

Then, the flow vector $\mathbf{U}_b$ has to be transformed into the geodetic system using $\mathbf{M}_{gb}$ (Haering, 1990; Leise and Masters, 1993; Boiffier,

1998). Finally the resulting $\mathbf{W}_g$ has to be transformed into the standard meteorological frame of reference, with the wind components u, v and w (east-, north- and upwards, respectively, Lenschow 1986).

$$
\begin{aligned}
u = v_g = v_{Ag} - |\mathbf{U}_a| D^{-1} \Big[& (\cos\Theta \cdot \sin\Psi) \\
& + \tan\beta \cdot (\sin\Phi \cdot \sin\Theta \cdot \sin\Psi + \cos\Phi \cdot \cos\Psi) \\
& + \tan\alpha \cdot (\cos\Phi \cdot \sin\Theta \cdot \sin\Psi - \sin\Phi \cdot \cos\Psi) \Big] \quad , \\
v = u_g = u_{Ag} - |\mathbf{U}_a| D^{-1} \Big[& (\cos\Theta \cdot \cos\Psi) \\
& + \tan\beta \cdot (\sin\Phi \cdot \sin\Theta \cdot \cos\Psi - \cos\Phi \cdot \sin\Psi) \\
& + \tan\alpha \cdot (\cos\Phi \cdot \sin\Theta \cdot \cos\Psi + \sin\Phi \cdot \sin\Psi) \Big] \quad , \\
w = -w_g = -w_{Ag} + |\mathbf{U}_a| D^{-1} \Big[& (-1 \cdot \sin\Theta) \\
& + \tan\beta \cdot (\sin\Phi \cdot \cos\Theta) + \tan\alpha \cdot (\cos\Phi \cdot \cos\Theta) \Big] \quad ,
\end{aligned}
\tag{5}
$$

with inertial velocity vector $\mathbf{V}_g$ = (u_{Ag}, v_{Ag}, w_{Ag}) and the Euler (attitude) angles pitch Θ, true heading Ψ and roll Φ.

3.1 Calibration of the 5HP

The calibration of the 5HP was performed at the Pfleiderer Institute (Technical University Braunschweig), which provided an open wind tunnel capable of wind velocities up to 100 m s^{-1}. The 5HP was mounted on the M^{2}AV fuselage nose and calibrated at an airflow velocity of 22 m s^{-1} and at predefined airflow angles $\tilde{\alpha}$ and $\tilde{\beta}$ between -20° and $+20^\circ$. The measurement uncertainty of the wind tunnel velocity was $0.7\% \approx 0.2$ m s^{-1} (for the specified velocity of 22 m s^{-1}). The airflow angles were varied manually during the calibration with an uncertainty of 0.2°.

The wind tunnel angles $\tilde{\alpha}$ and $\tilde{\beta}$ are related to the airflow angles α and β (Boiffier, 1998) used for the wind calculation (5):

$$
\begin{aligned}
\alpha &= \tilde{\alpha} \quad , \\
\beta &= \arctan\left(\frac{\tan\tilde{\beta}}{\cos\tilde{\alpha}}\right) \quad .
\end{aligned}
\tag{6}
$$

The 5HP has five total pressure ports on its conical head and four static pressure ports downstream the head (Fig. 2). Five differential pressures are measured: the difference between the central hole and each of the four remaining total pressure ports (ΔP_{01}, ΔP_{02}, ΔP_{03}, ΔP_{04}) and the difference between the static pressure and the central hole (ΔP_{0s}). These measurements are used to determine a total pressure difference (Sasongko,

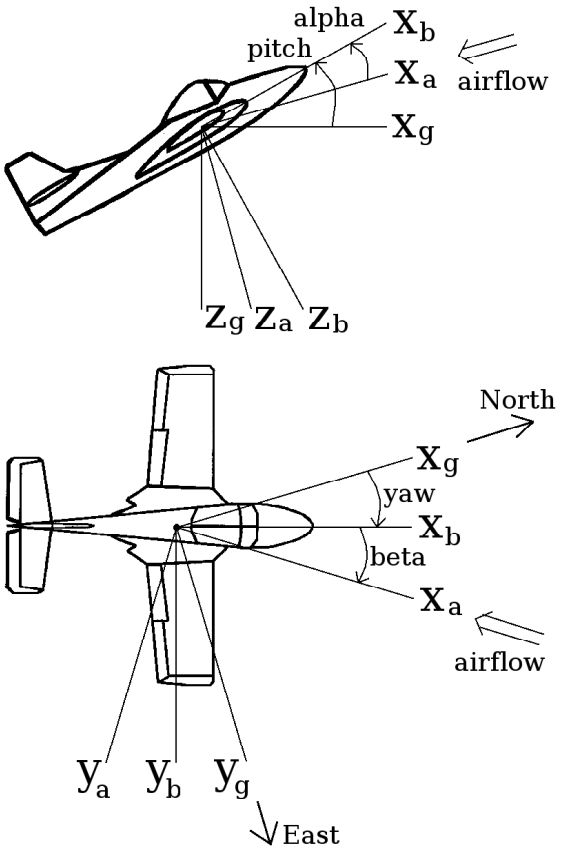

Fig. 3: *The three aircraft coordinate systems, aerodynamic (index 'a'), geodetic (index 'g') and body coordinate system (index 'b') needed for the wind calculation.*

1997)

$$
\Delta P = \left[\frac{1}{5} \sum_{i=0}^{4} \left(P_i - \frac{1}{5} \sum_{j=0}^{4} P_j \right)^2 \right]^{\frac{1}{2}} + \left[P_0 - \frac{1}{4} \sum_{i=1}^{4} P_i \right] \quad , \tag{7}
$$

which can be calculated by the individual pressure differences.

Dimensionless pressure coefficients k_α and k_β are defined using ΔP and the measured differential pressures

$$
k_\alpha = \frac{\Delta P_{01} - \Delta P_{03}}{\Delta P} \quad , \tag{8}
$$

$$
k_\beta = \frac{\Delta P_{02} - \Delta P_{04}}{\Delta P} \quad . \tag{9}
$$

To calculate the airflow angles and the dimensionless coefficient k_q for the dynamic pressure, three functions were defined

$$
\begin{aligned}
\tilde{\alpha} &= f_1(k_\alpha, k_\beta) \quad , \\
\tilde{\beta} &= f_2(k_\alpha, k_\beta) \quad , \\
k_q &= f_3(k_\alpha, k_\beta) \quad ,
\end{aligned}
\tag{10}
$$

with the general calibration polynomial form (11th order for both m and n) for f_x ($x = 1, 2$ or 3) according to Bohn and Simon (1975)

$$f_x(k_\alpha, k_\beta) = \sum_{i=0}^{m} (k_\alpha)^i \left[\sum_{j=0}^{n} X_{ij} (k_\beta)^j \right] \quad , \qquad (11)$$

where X_{ij} represents the coefficients for the angle of attack a_{ij}, sideslip angle b_{ij} or dynamic pressure q_{ij} for f_1, f_2 and f_3 respectively. The function (11) contains $m \cdot n$ unknown coefficients which can be determined with a system of $m \cdot n$ independent equations. This linear problem is solved by the least square method for all three functions (10) and returned the coefficients a_{ij}, b_{ij} and q_{ij}.

The method enabled the determination of the airflow angles and the dynamic pressure coefficient k_q with the measurements of the 5HP. Finally the dynamic pressure q during flight is calculated

$$q = \Delta P_{0s} + \Delta P \cdot k_q \quad , \qquad (12)$$

and used to calculate the true airspeed (4).

3.2 GPS-INS fusion

The reliable determination of attitude, velocity and position of the aircraft is essential for wind identification. With the M^{2}AV this is achieved by an integrated navigation system consisting of a GPS and an INS. The INS calculates the position, velocity and attitude by a strap-down calculation of the accelerations and angular rates measured by the IMU. The GPS/INS system offers a significantly increased performance, compared to a INS only, due to the complementary characteristics of GPS and INS, where the latter assures the continuous availability of the attitude, velocity and position. The growth of navigation errors with time due to the low cost MEMS IMU is prevented by the use of aiding information provided by the GPS receiver. Figure 4 displays the navigation-filter architecture.

For the GPS/INS integration a discrete error state Kálmán Filter was used (Gelb, 1989). Kálmán filters are based on linear dynamic systems discretize in the time domain (Kálmán, 1960). The system model uses the following discrete error-state vector: three position-, three velocity- and three attitude-errors as well as three errors in the gyro sensor signal bias, three errors in the accelerometer signal bias, one error in the GPS receiver clock error and one error in the clock drift, which are in total 17 states. By processing GPS raw data (pseudo range, delta range and carrier phase), estimates of the error-state vector are

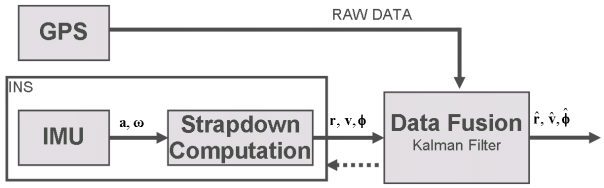

Fig. 4: *Navigation filter structure where* **a** *and* ω *are the accelerations and the angular rates from the IMU,* **r**, **v** *and* ϕ *the position, velocity and attitude from the INS system. The position, velocity and attitude solution from the Kálmán filter are defined as* $\hat{\mathbf{r}}$, $\hat{\mathbf{v}}$ *and* $\hat{\phi}$.

made which corrects the full states of the navigation system. The GPS receiver measures the delay of the satellite signal and calculates the distance to the satellite, which is called the pseudo range. The delta range is the velocity of the GPS receiver relative to the satellite calculated via Doppler shift of the carrier wave. The receiver gives also the phasing of the carrier wave. This method of aiding is called tightly coupled (Wendel and Trommer, 2004). Furthermore, with such a filter the INS can still be aided by GPS when there are less than four visible satellites. A tightly-coupled GPS/INS filter usually processes pseudo ranges and delta ranges. Based on the method used by Farrell (2001) and van Graas and Farrell (2001), the delta ranges can be replaced by time-differenced carrier phases and used for the M^{2}AV navigation (Winkler and Vörsmann, 2007). It was proofed that the filter with time-differenced carrier phase achieved a better velocity and attitude accuracy than the filter using delta-ranges. The method allows using the high measurement accuracy of the carrier phase without solving the integer ambiguities. Compared to a delayed state Kálmán filter (which would be commonly used in such case) this method does not induce additional cross-correlation between measurements at one epoch.

3.3 In-flight wind calibration

The wind vector (5) calculated from airborne measurements is very sensitive to errors in the input parameters. The first M^{2}AV data sets were measured in both convective and neutral stratification (over land, near Braunschweig, Germany). During these flights the mean vertical wind was expected to be nearly zero, but the actually measured $\overline{w}$ showed a deviation of a few m s^{-1}. The mean horizontal wind components were assumed to be constant during the entire flight. However both measured u and v time series showed

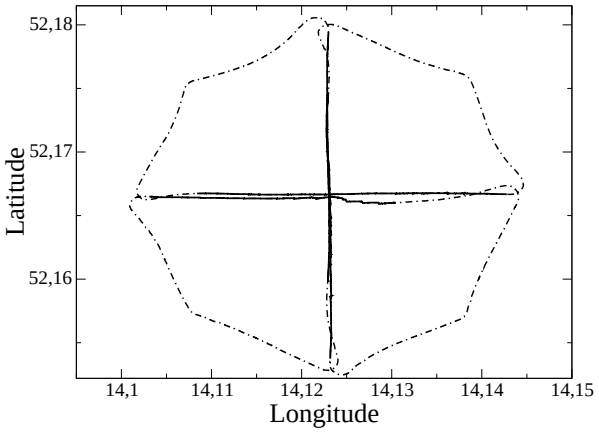

Fig. 5: *Star flight pattern performed on 1 August, 2007, the dashed-dotted line represents the complete flight, the solid lines the horizontal legs used for the in-flight calibration.*

offsets depending on the flight direction compared to $\overline{u}$ and $\overline{v}$ for a complete square-shaped pattern. The origin of these deviations were analyzed by van den Kroonenberg *et al.* (2008) which resulted in the determination of two correction angles $\Delta\Psi'$, $\Delta\Theta'$ and the correction factor for the true airspeed f_{U_a}.

These corrections can be determined during an in-flight calibration flying a 'star' pattern (Fig. 5). The ideal atmospheric conditions for the in-flight calibration are no large turbulent transport, a constant mean horizontal wind and a mean vertical wind near zero. For every straight horizontal leg the mean values ($\overline{\mathrm{U}}_a, \overline{\alpha}, \overline{\beta}, \overline{\Theta}, \overline{\Psi}, \overline{\Phi}, \overline{u}_{Ag}, \overline{v}_{Ag}, \overline{w}_{Ag}$, uncorrected) will be calculated from the measured time series. These mean values will be used to calculate the mean wind vector using equation (5) which is supplemented by the unknown correction factors. The following parameter are replaced in (5)

$$\begin{aligned} \Theta &\Rightarrow \overline{\Theta} + \Delta\Theta' \quad , \\ \Psi &\Rightarrow \overline{\Psi} + \Delta\Psi' \quad , \\ \mathbf{U}_a &\Rightarrow \overline{\mathbf{U}}_a \cdot f_{\mathrm{U}_a} \quad , \end{aligned} \tag{13}$$

where $\overline{\Theta}$, $\overline{\Psi}$ and $\overline{\mathbf{U}}_a$ are the mean values of the pitch angle, true heading and the true airspeed, respectively.

The assumptions that the mean horizontal wind components are actually identical on a round trip (two identical legs flown in reverse direction) and the mean vertical wind is close to zero, leads to

Tab. 2: *Measurement flights performed at Antarctica 2007. A 3D-box are several square-shaped pattern (1 km x 1 km) in different altitudes. The wide-box is a larger rectangular-shaped pattern (5 x 0.7 km at Halley station and 15 x 2 km at Windy Bay).*

flight no.	date dd-mm	pattern	altitude m (agl)
01	30-10	3D-box	195, 250
02	01-11	-	*flight aborted*
03	02-11	3D-box	230, 250
04	02-11	3D-box, star	165, 185
05	05-11	3D-box, star	136, 170, 190
06	05-11	3D-box	155, 188
07	14-11	wide-box[2]	100, 120, 140
08	15-11	wide-box[2]	70, 80
09	22-11	3D-box, star	65, 85
10	22-11	wide-box[2]	85, 95, 120
11	22-11	wide-box[2]	60, 80, 100
12	23-11	3D-box, star	90, 145
13	28-11	wide-box	50, 80, 130
14	28-11	wide-box	50, 75, 130
15	29-11	3D-box, star	48, 55
16	29-11	3D-box, star	30, 36
17	30-11	wide-box	50, 80, 130
18	01-12	wide-box	60, 85, 140
19	01-12	wide-box	55, 82, 135
20	01-12	3D-box, star	44, 50
21	02-12	wide-box	54, 82, 130

the following set of equations

$$\begin{aligned} \overline{u}^n - \overline{u}^s = 0, \quad \overline{v}^n - \overline{v}^s = 0 \quad , \\ \overline{u}^w - \overline{u}^e = 0, \quad \overline{v}^w - \overline{v}^e = 0 \quad , \\ \overline{w}^n = \overline{w}^s = \overline{w}^w = \overline{w}^e = 0 \quad , \end{aligned} \tag{14}$$

where n, s, w and e indicate north, south, west or east flight direction.

The unknown angles $\Delta\Psi'$, $\Delta\Theta'$ and f_{U_a} are calculated from (14) where u, v and w are calculated by (5) using the substitutions from (13). The Levenberg-Marquardt least squares fit method (Press *et al.*, 1992) is used to solve the equations.

3.4 M²AV measurements at Halley V

Since 2005 M²AV are in deployment at Halley V on the Brunt Ice Shelf in the Weddell Sea of Antarctica. The surrounding area of Halley is flat ice and the station is located in an ellipse of the

[2] Wide-box pattern (15 x 2 km) flown at Windy Bay, 18 km North-West of Halley V station

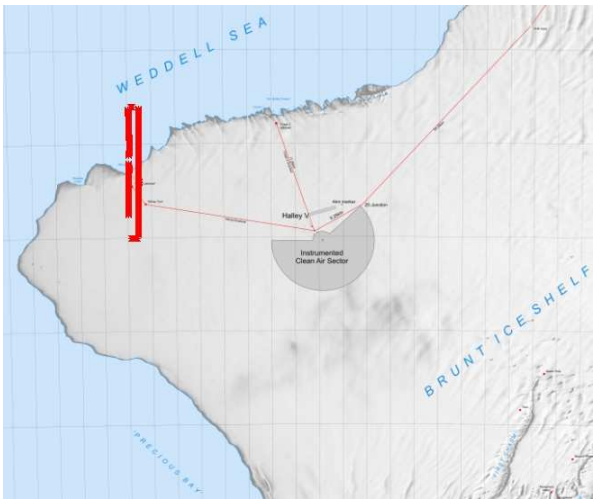

Fig. 6: *A wide-box flight pattern performed on November, 22, 2007 at Windy Bay and the location of Halley V station.*

coastline, about 15 km for the coast to the north, west and south-west. At Halley several experiments are carried out continously. Ozone and other trace gases are measured at the clean air sector laboratory (CASLab). A single axis vertically pointing acoustic sounder (sodar) measures the acoustic backscatter in the atmosphere up to 500 m. Turbulence measurements are performed at several heights on a 32 m mast close to the CASLab and further standard meteorological measurements in 2 m and 10 m are taken at the main station. Radio sonde are launched once per day and in springtime further basic meteorological and ozone data are taken occasionally using a thetered balloon.

Due to the bad weather conditions at Halley in the summer and autumn 2007 no meteorological flights were made. During this period the systems were tested and modified for the cold temperatures. The meteorological flights started end of October, 2007. In total 20 flights were performed from which 4 were off- base (Tab. 2). The on-site flights were performed at Halley station near the sodar and the 32m-tower. The off-base flight were performed at Windy Bay, crossing the shelf-ice edge.

4. RESULTS

Four flights were chosen for this comparison study (Tab. 3). These flights were chosen while the M^{2}AV flew particularly low and therefore comparable with the tower measurements at Halley station. A direct comparison with the tower was not possible while for safety reason the highest tower level of 32 m above ground could not be reached with the M^{2}AV .

Tab. 3: *The horizontal wind speed U_{hor} and the wind direction Ω_{hor} are listed for the flight no. 09, 15, 18 and 19. σ represents the standard deviation of the measurements.*

flight no.	time UTC	z m	U_{hor} (σ) m s^{-1}	Ω_{hor} (σ) deg
09	11:20	81	5.2 (0.6)	60.6 (9.4)
09	11:26	85	4.9 (0.4)	67.2 (6.6)
09	11:30	63	5.7 (0.3)	59.9 (2.8)
15	15:33	52	2.5 (0.3)	78.9 (8.7)
15	15:42	54	2.3 (0.3)	71.0 (4.6)
15	15:46	48	2.2 (0.3)	71.0 (0.9)
18	15:58	134	5.2 (0.7)	66.5 (48.2)
18	16:06	83	4.0 (0.9)	80.2 (32.0)
18	16:14	59	3.2 (0.3)	77.0 (17.8)
18	16:20	59	3.1 (0.1)	87.3 (1.6)
19	16:53	113	2.5 (0.2)	70.7 (6.5)
19	16:59	131	3.1 (0.3)	78.0 (31.6)
19	17:07	82	4.0 (0.4)	75.4 (51.9)
19	17:16	54	3.0 (0.4)	71.8 (30.6)
19	17:20	53	2.4 (0.2)	77.9 (3.9)

The calibration 'star' flights were used to calculate the correction angles $\Delta\Psi'$, $\Delta\Theta'$ and the correction factor f_{U_a}. The mean wind components were calculated for each square- or rectangular-shaped pattern at a certain altitude (using the correction angles and factor). For comparison the sonic measurements (10 min average) were selected for the same time period at all levels: 1, 2, 4, 8, 16 and 32 m above ground.

Figures 7-8 show that the M^{2}AV wind speed and direction measurements agreed well with the extrapolated tower data. The standard deviation of the wind speed for both days had a maximum of 1 m s^{-1} and for the wind direction a maximum of 10 deg (Tab. 3).

Figure 9 shows the results of two flights performed consecutively on the same day. The wind speed agreed well with the tower measurements. The wind direction shows much larger standard deviations compared to the first two days, nevertheless, the mean values agree with the tower measurements.

4.1 Temperature

Figure 10 shows the temperature profiles com-

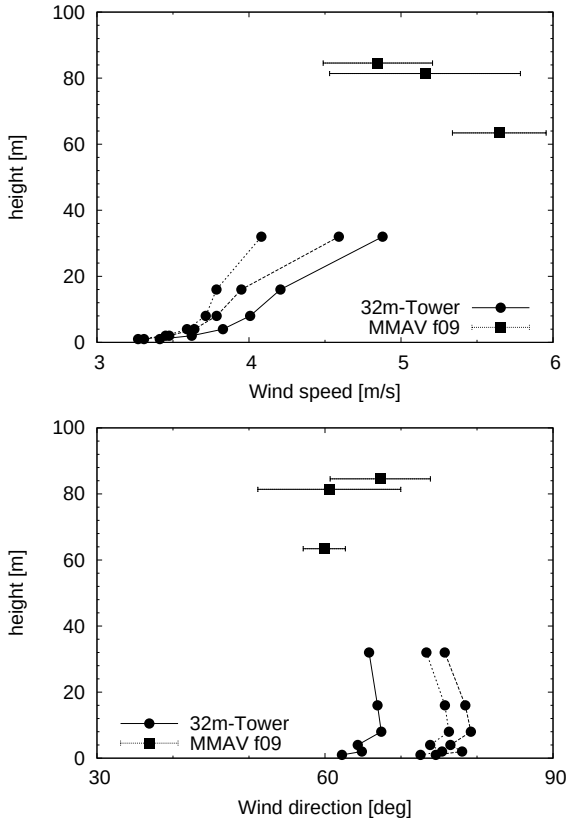

Fig. 7: *Flight 09 (11:14 - 11:32 UTC). Top: wind speed. Bottom: wind direction. The error bars represent the standard deviations of the M²AV measurements.*

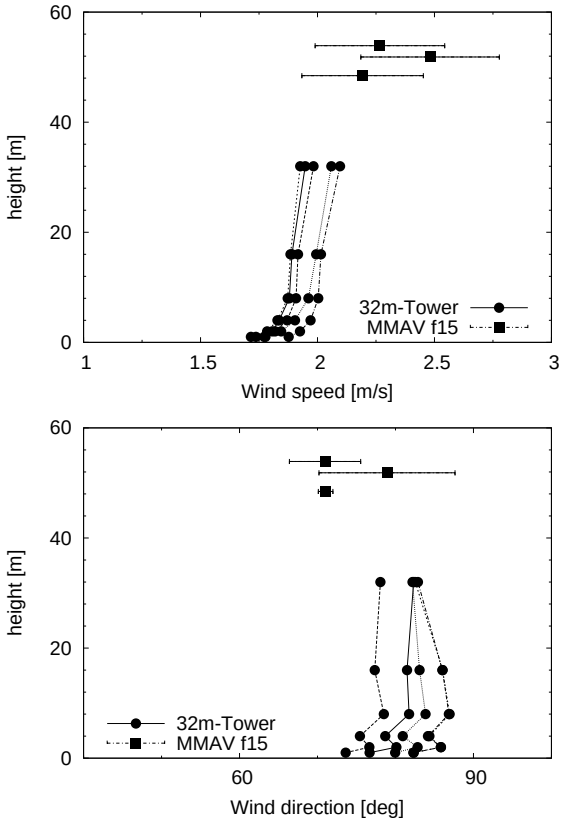

Fig. 8: *Flight 15 (15:24 - 15:48 UTC). Top: wind speed. Bottom: wind direction*

pared with the 10 min averaged tower data. On both days, a very shallow (5 m thick) inversion at the surface was measured by the tower. Above this layer the temperature strongly decreased till 30-40 m above surface level. The layer above showed an adiabatic temperature decrease (visible for flights 18 and 19) which could be some kind of a residual layer.

5. CONCLUSIONS

The M²AV was developed as a low-cost and easy-to-handle system for boundary-layer research that has not to be remotely controlled by a pilot on the ground but operates autonomously. The advantages of the auto-pilot are the possibilities to fly out of sight (long distance flights) or at night (stable boundary layer research). At a typical airspeed of 22 m s^{-1} the M²AV can reach a flight distance of $60 - 70$ km. It was not intended to compete with large and heavy airborne research systems (for instance like the Helipod, Bange and Roth, 1999) in means of data accuracy. Nevertheless, the results are quite promising since the systematic measurement errors (mainly caused by the use of light, small and inexpensive sensors) are acceptable small.

ACKNOWLEDGMENT

The data analysis is funded by the German Science Foundation DFG (FSA: Fine Structure of the Stably Stratified Atmospheric Boundary Layer in Antarctica, within “Schwerpunktprogramm 1158 Antarktisforschung”, grant no. Ba 1988/4-1).

REFERENCES

Axford, D. N., **1968**: On the Accuracy of Wind Measurements Using an Inertial Platform in an Aircraft, and an Example of a Measurement of the Vertical Mesostructure of the Atmosphere. *J. Appl. Meteor.*, **7**, 645–666.

Bange, J. and **Roth, R.**, **1999**: Helicopter-Borne Flux Measurements in the Nocturnal Boundary Layer Over Land - a Case Study. *Boundary-Layer Meteorol.*, **92**, 295–325.

Bange, J., **Beyrich, F.** and **Engelbart, D. A. M.**,

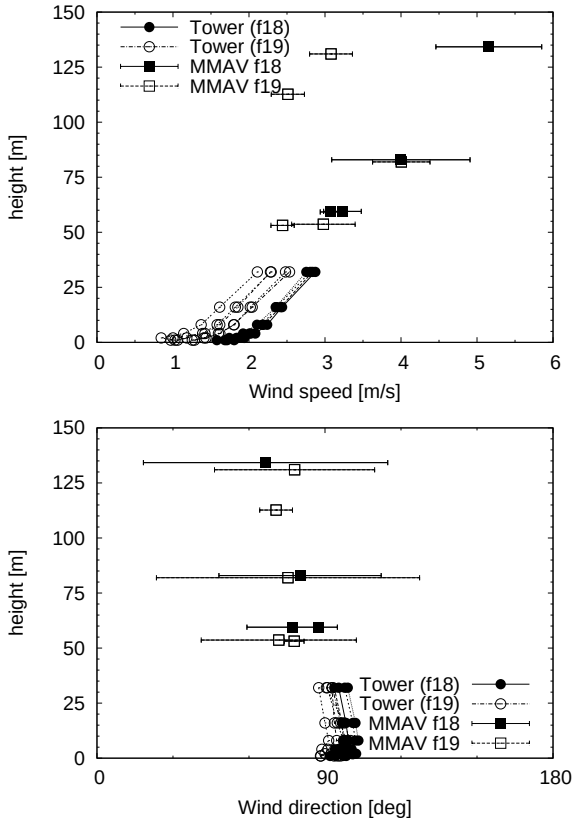

Fig. 9: *Flight 18 (15:53 - 16:23 UTC) and 19 (16:51 - 17:23 UTC). Top: wind speed. Bottom: wind direction*

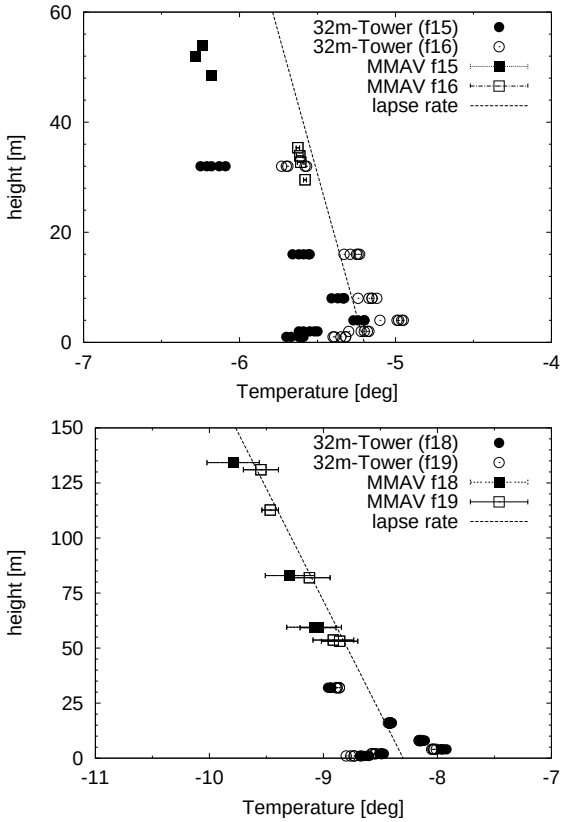

Fig. 10: *Temperature compared to the tower measurements (10 min averages) The dashed line represents the adiabatic lapse rate. Top: Flight 15 - 16 performed on November, 29, 2007. Bottom: Flight 18 - 19 performed on December, 1, 2007.*

2002: Airborne Measurements of Turbulent Fluxes during LITFASS-98: A Case Study about Method and Significance. *Theor. Appl. Climatol.*, **73**, 35–51.

Beyrich, F. and **Mengelkamp, H.-T.**, **2006**: Evaporation over a Heterogeneous Land Surface: EVA_GRIPS and the LITFASS-2003 Experiment - an Overview. *Bound.-Layer Meteor.*, **121**, 1–28.

Bohn, D. and **Simon, H.**, **1975**: Mehrparametrige Approximation der Eichräume und Eichflächen von Unterschall- bzw. Überschall-5-Loch-Sonden. *ATM, Bd. 42*, **3**, 31–37.

Boiffier, J.-L., **1998**: *The Dynamics of Flight – the Equations*. Wiley, Chichester, UK, 353 pp.

Buschmann, M., **Bange, J.** and **Vörsmann, P.**, **2004**: M^2AV- A Miniature Unmanned Aerial Vehicle (MINI-UAV) for Meteorological Purposes. In: *16th Symposium on Boundary Layers and Turbulence*, AMS, Portland/Maine, USA, 6.7.

Farrell, J. L., **2001**: Carrier phase processing without integers. In: *the Institute of Navigation 57th Annual Meeting*, ION, Albuquerque, NM, pp. 423–428.

Gelb, A. H., **1989**: *Applied Optimal Estimation*. The M.I.T.. Press, Cambridge, MA, London.

van Graas, F. and **Farrell, J. L.**, **2001**: GPS/INS - a very different way. In: *the Institute of Navigation 57th Annual Meeting*, ION, Albuquerque, NM, pp. 715–721.

Grossman, R. L., **1977**: A Procedure for the Correction of Biases in Winds Measured from Aircraft. *J. Appl. Meteor.*, **16**, 654–658.

Haering, E. A., **1990**: Airdata Calibration of a High-Performance Aircraft for Measuring Atmospheric Wind Profiles. Tech. Mem. 101714, NASA, 24 pp.

Kálmán, R. E., **1960**: A new approach to linear filtering and prediction problems. *Trans. ASME, J. Basic Eng.*, **82**, 35–45.

van den Kroonenberg, A. C., **Martin, T.**, **Buschmann, M.**, **Bange, J.** and **Vörsmann, P.**, **2008**: Measuring the Wind Vector Using the Autonomous Mini Aerial Vehicle M^2AV. *J. Atmos. Oceanic Technol.*, accepted for publication.

Leise, J. A. and **Masters, J. M.**, **1993**: *Wind measurements from aircraft*. US Department of Commerce, National Oceanic and Atmospheric Administration, Aircraft Operation Center, Miami, Florida, USA, 166 pp.

Lenschow, D. E., **1986**: *Probing the atmospheric boundary layer*. American Meteorological Society, 289 pp.

Press, W., **Flannery, B.**, **Teukolsky, S.** and **Vetterling, W.**, **1992**: *Numerical recipes in C: The art of scientific computing*. Cambridge University Press, 1020 pp.

Sasongko, H., **1997**: *Rand- und Spaltströmungen in stark gestaffelten Verdichtergittern aus schwach gewölbten Profilen*. No. 1997-01 in ZLR-Forschungsbericht, Technische Universität Braunschweig.

Spieß, T., **Bange, J.**, **Buschmann, M.** and **Vörsmann, P.**, **2007**: First Application of the Meteorological Mini-UAV 'M^{2}AV'. *Meteorol. Z. N. F.*, **16**(2), 159–169.

Wendel, J. and **Trommer, G. F.**, **2004**: Tightly coupled GPS/INS integration for missile applications. *Aerospace Science and Technology*, **8**, 627–634.

Winkler, S. and **Vörsmann, P.**, **2007**: Multi-Sensor Data Fusion for Small Autonomous Unmanned Aircraft. *Eurpean Journal of Navigation*, **5**(2), 32–41.